Desalination and Water Treatment
www.deswater.com

doi: 10.5004/dwt.2017.20288

65 (2017) 313–326
February

Optimization and mechanism study of C.I. Acid Blue 25 wastewater degradation by ozone/Fenton oxidation process: response surface methodology, intermediate products and degradation pathway

Yongjun Shen*, Qihui Xu, Jiaming Shi, Mi Li, Yan Zhang

School of Chemistry and Chemical Engineering, Nantong University, Nantong 226019, China, emails: shenyj@ntu.edu.cn (Y. Shen), 2360560873@qq.com (Q. Xu), wodeziliao1@163.com (J. Shi), wodeziliao998@163.com (M. Li), zhangyan@ntu.edu.cn (Y. Zhang)

Received 4 May 2016; Accepted 24 October 2016

ABSTRACT

Degradation process of C.I. Acid Blue 25 by the combined ozone and Fenton (O_3/Fenton) system was investigated. The Box-Behnken design and response surface methodology were applied in designing the experiments for evaluating the interactive effects of the three most important operating variables. The results demonstrated that the optimal operating conditions were pH of 5.48, $[H_2O_2]/[Fe^{2+}]$ of 45.47, c_0 of 55.08 mg.L^{-1} and $q_{(O3)}$ of 42.06 L.h^{-1}. Under conditions above, 96.67% decolorization rate of C.I. Acid Blue 25 could be obtained after 4 min reaction time. By validating the results through parallel experiment, the decolorization rate reached 96.39%, and the deviation with the model prediction was only 2.90%. In addition, the highest removal rate of chemical oxygen demand was higher than 85% after 20 min. Main reaction intermediate products involving *p*-benzoquinone, aniline, catechol, hydroquinone etc. were determined by analyses of ultraviolet-visible spectroscopy, Fourier transform infrared spectroscopy and gas chromatography/mass spectrometry (GC/MS). Based on the results of analyses above, the possible degradation pathways of C.I. Acid Blue 25 by O_3/Fenton system were proposed.

Keywords: Ozone/Fenton; Response surface methodology; Intermediate products; Mechanism; C.I. Acid Blue 25

1. Introduction

Textile processes (dyeing, bleaching, printing and finishing) required large water consumption in industry, which produced a great amount of wastewater [1]. Textile wastewater comprised a variety of dyes and chemicals that made the chemical composition of textile industry effluents an environmental challenge [2]. As a result, a large amount of wastewater with poor quality not only caused esthetic problems but could also be dangerous, because dyes and their by-products were very toxic to environment [3]. Therefore, proper treatment of dyes containing textile effluent before discharge was extremely necessary [4]. In recent years, normal treatment methods of dye wastewater have been analyzed, mainly including common methods such as coagulation [5], activated carbon adsorption [6], physical adsorption method [7], biochemical method [8] such as activated sludge [9], and electrochemical method [10,11]. But traditional wastewater treatment technologies were proven to be markedly ineffective for handling that wastewater because of the toxicity and slow degradation of the dyes [3,12,13]. The application of advanced oxidation processes (AOPs) to environmental issues has attracted considerable attention [14–16]. AOPs could completely decompose the organic pollutants with the less activity in aqueous solution quickly and non-selectively by generation of reactive species including hydroxyl radicals [17–19], such O_3 [20], O_3/H_2O_2 [21], Fenton [22], ultraviolet (UV) [23], ultrasonic [24] and plasma [25,26].

As one of the AOPs, Fenton reaction was an effective method of mineralizing recalcitrant pollutants in industrial wastewaters [27]. Fenton utilized the strong oxidation potential of the free radicals to oxidize and remove pollutants. However, pH had the great influence on Fenton treating

* Corresponding author.

wastewater [28]. In addition, ozone-based AOPs involving the generation of the hydroxyl radicals (·OH), which were highly reactive with most organic compounds, could be widely used in dye industrial areas [29]. Thus, O_3 could be chosen to combine with Fenton to enhance removal efficiency, which was a promising technology for contaminant removal from wastewater.

For practical application, it was important to optimize the experimental conditions in order to develop a cost-effective O_3/Fenton process. Thus, response surface methodology (RSM) could be used to study degradation process [2,30]. Martí-Calatayud et al. [31] agreed that RSM was an effective instrument that could be widely used to analyze the effects of multiple factors and their interaction. It made the overall optimization of the process feasible. In addition, when Yang et al. [32] applied hybrid coagulants and polyacrylamide flocculants to treat high-phosphorus hematite flotation wastewater, RSM was also used as an empirical statistical modeling technique to design experiments, to build models, to evaluate the effects of several factors, and to search optimum conditions for desirable response, with limited number of planned experiments.

Moreover, because the dye may be toxic, in order to avoid the problem that the toxicity of dye intermediate products could be greater during degradation process, elucidating oxidation mechanism would also be an essential and practicable way to study the degradation process, concretely through the ways of characterizing reaction products and suggesting the potential pathway [33]. However, few works have fulfilled organic pollutant degradation based on analyzing mechanism of intermediate products letting alone in O_3/Fenton system. And few comprehensive studies that involved optimization by RSM, mechanism analysis of intermediate products and degradation pathway have been found in the literature about degradation of C.I. Acid Blue 25.

In this paper, the objectives were to investigate degradation process of the C.I. Acid Blue 25, which was selected as the example of contaminants from multiple perspectives in O_3/Fenton system. The decolorization rate and the removal rate of chemical oxygen demand (COD) were detected, respectively. The RSM based on Box- Behnken design (BBD) was employed to evaluate the effects of the key variables, i.e., the initial pH, molar ratio of $[H_2O_2]/[Fe^{2+}]$, the concentration of dye and ozone flux. The quadratic polynomial equation was developed with the experimental datum. The optimal O_3/Fenton reaction conditions were obtained and validated. In addition, main reaction intermediates, and products of the C.I. Acid Blue 25 were detected by gas chromatography/mass spectrometry (GC/MS) during the degradation process in O_3/Fenton system. The formation mechanisms of main intermediate compounds were discussed in detail as much as possible, and every step with detailed chemical reaction equations was provided. Eventually, a general potential pathway of the C.I. Acid Blue 25 degradation was suggested.

2. Experimental setup

2.1. Materials

All the chemicals used were of analytical grade. The C.I. Acid Blue 25 (Shanghai Jiaying Co., Ltd., China) was used as dye pollutants. Its molecular formula was $C_{20}H_{13}N_2NaO_5S$. Fenton reagent involved granular ferrous sulfate ($FeSO_4.7H_2O$) (Merck KGaA, Germany) and hydrogen peroxide solution (30%, w/w) (Merck KGaA, Germany). The acidic potassium permanganate (Shantou Xilong Chemical Co., Ltd., China) would be used under the process of detecting COD values. NaOH (Shanhai Chemical Co., Ltd., China) or H_2SO_4 (Shantou Xilong Chemical Co., Ltd., China) was used to adjust suitable pH to a certain value.

2.2. Experimental procedure

Dye solutions were prepared with distilled water. The schematic diagram of O_3/Fenton system was depicted in Fig. 1. Ozone was generated by electrical discharge using oxygen in a laboratory ozone generator (WH-K-3.5, Jiangsu Nanjing Wohuan Technology Co., China), and the total output of ozone was 3.5 $g.h^{-1}$ before ozone entering glass rotameter. Then, the ozone-oxygen mixture was continuously bubbled into the solution. The flux rate was controlled by glass rotameter. At the same time, certain quantity of $FeSO_4.7H_2O$ (0.16, 0.04, 0.02, 0.01 and 0.005 g) was added into the dye wastewater, and then hydrogen peroxide solution (30%, w/w; 0.3 mL) was added to initiate the reaction ($[H_2O_2]/[Fe^{2+}]$ = 20:1, 0.01 g $FeSO_4.7H_2O$ and 0.075 mL 30% H_2O_2). In addition, the mixture of the solution was provided by a magnetic stirrer (85-2, Jintai Technology Co., China). The specific

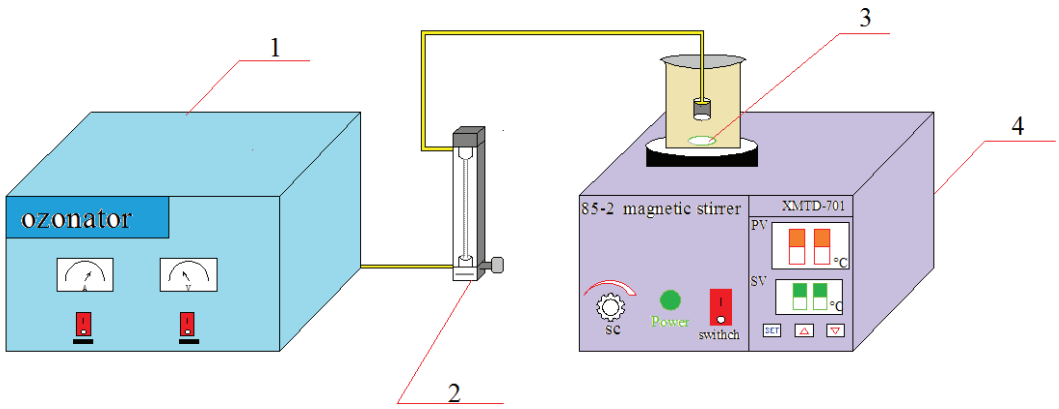

Fig. 1. Installation drawing on the degradation of C.I. Acid Blue 25 by O_3/Fenton systems.
Note: 1 – ozonator, 2 – rotameter, 3 – rotor, and 4 – magnetic stirrer.

Table 1
Experimental range and levels of independent variables

Variables	Symbols	Range and level		
		Low (–1)	Center (0)	High (+1)
pH	X_1	1	6.5	12
Mole ratio ($[H_2O_2]/[Fe^{2+}]$), mol/mol	X_2	20	90	160
Initial concentration, mg.L^{-1}	X_3	20	110	200
Ozone flux, L.h^{-1}	X_4	16	38	60

experimental parameters involving pH, the mole ratio of $[H_2O_2]/[Fe^{2+}]$, initial concentration of dye and ozone flux for all O_3/Fenton experiments were listed in Table 1.

2.3. Characterization of degradation sample

2.3.1. Decolorization rate and removal rate of COD

The concentration of sample was determined at regular intervals by using an ultraviolet spectrophotometer (752N, Shanghai Shunyu Hengping Technology Co., China) at the maximum absorption wavelength of 609 nm. The decolorization rate (η) was calculated according to Eq. (1):

$$\eta = \frac{c_0 - c_t}{c_0} \times 100\% \quad (1)$$

where the c_0 and c_t were the absorbency of the sample at time 0 and t, respectively.

Accordingly, the COD value was measured by the acidified potassium permanganate index method [34]. Similarly, the removal rates of COD before and after treatment were evaluated by Eq. (1) to investigate the degradation efficiency of the C.I. Acid Blue 25 wastewater solution.

2.3.2. UV-Vis

Ultraviolet-visible (UV-Vis) method was an analytic method of the material electron spectrum. The spectral region ranged from 200 to 800 nm when radiation was absorbed by certain substance molecular. The absorption spectra of electronic energy level transitions were the result of electron energy level transition between valence electrons and molecular orbital. Determining the absorption of the molecular under UV-Vis method could authenticate and quantitatively determine a large amount of inorganic compounds and organic compounds.

2.3.3. FT-IR

The Fourier transform infrared (FT-IR) spectroscopy was used to detect the functional groups of the materials. By using KBr disk technique, the FT-IR spectra of the raw and activated samples were obtained with a FTS 6000 FT-IR spectrometer in the range of 4,000–400 cm^{-1}. The C.I. Acid Blue 25 (10 mg.L^{-1}) was prepared and degraded by O_3/Fenton. The samples were well blended with KBr and then desorbed at room temperature and eventually pressed to obtain IR-transparent pellets.

2.3.4. GC/MS

In order to identify intermediate products during degradation process of C.I. Acid Blue 25, GC/MS (VARIAN 450-GC/320-MS) analyses were performed. The solution of C.I. Acid Blue 25 was extracted with dichloromethane for 10 times, and then the extracts were concentrated by rotary evaporator at 313 K to about 1 mL before GC/MS analyses. A VF-5 MS capillary column (30 m length, 0.25 mm inner diameter, 0.25 μm film thickness) was used for GC separation. The GC equipment were operated in a temperature programmed mode with an initial temperature of 308 K held for 2 min, then ramped to 553 K with a 283 K.min^{-1} rate. Helium was used as the carrier gas at a flux rate of 0.9 cm^3.min^{-1}, and the pressure in the column head was 100 kPa. Then, electron impact (EI) mass spectra was scanned. The temperature of the MS transfer line was 553 K. The MS source temperature was 503 K. The MS quadrupole temperature was 423 K, and ionization was performed by electron ionization at 70 eV.

3. Results and discussion

3.1. Spectrum analysis of C.I. Acid Blue 25

3.1.1. UV-Vis spectrum analysis

As could be seen from Fig. 2(a), the waveform showed that the simulated C.I. Acid Blue 25 wastewater had four main peaks at 0 min. It indicated that the C.I. Acid Blue 25 in the UV region (200–400 nm) had two characteristic absorption peaks at 250 and 285 nm, which corresponded to the characteristic absorption peaks of aromatic compounds. In the visible region (400–800 nm), there were also two characteristic absorption peaks. One was at 410 nm, and the other was broad peak (609–653 nm). The peak at 410 nm was due to the conjugated system of carbonyl and benzene. The broad peak (609–653 nm) was caused by anthraquinone chromophoric group. The anthraquinone groups made the whole dye molecules present the unique green. The peak value abated after 5 min. And the visible broad peak appeared a dramatic change. Then, the peak disappeared synchronously along with the phenomenon that the dye faded away. It showed that anthraquinone group was attacked by the strong oxidation of ·OH and was completely destroyed. ·OH played a role in the open loop and chain scission. With the extension of oxidation time, small molecules such as CO_2 and H_2O were generated, and the color of the dye was faded.

3.1.2. FT-IR spectrum analysis

It could be seen from Fig. 2(b) that the sample at 1,568–1,458 cm^{-1} was the C=C stretching vibration absorption peak of typical skeleton of benzene ring. It usually had four peaks, but the four peaks did not always appear at the same time. The peaks at 1,039, 1,073 and 3,445 cm^{-1}, respectively, corresponded to –SO_3Na vibration, C=O stretching vibration and –NH vibration. The vibration absorption peak of C=C band of benzene ring skeleton appeared at 1,643 cm^{-1} after 30 min of degradation, namely the peak was moved to takanami. It indicated that a great conjugated system of the molecules had become a relatively small benzene ring system. The characteristic peak of –SO_3Na shifted to 1,137 cm^{-1},

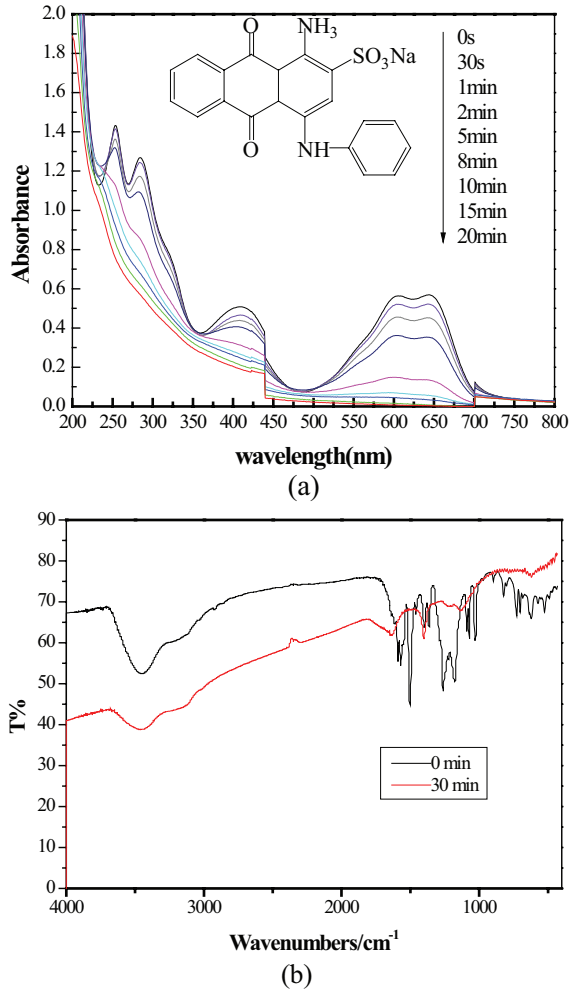

Fig. 2. (a) UV-Vis absorption spectrum of C.I. Acid Blue 25 at different degradation time and (b) infrared spectroscopy of before and after degradation of C.I. Acid Blue 25.

and the characteristic peak of –NH shifted to 3,448 cm^{-1}. Despite the existence of the peak type, the amplitude of the peak was greatly reduced. The C=O peak disappeared, which demonstrated that it had already been attacked by ·OH. For anthraquinone dyes, once the C=O band was broken, its adjacent benzene ring would be easily oxidized to open loop.

3.2. Degradation analysis of C.I. Acid Blue 25

3.2.1. Effect of initial pH

The effects of different initial pH of C.I. Acid Blue 25 on the treatment of O_3/Fenton were seen in Fig. 3(a). When the initial pH increased, the decolorization rate of C.I. Acid Blue 25 and the removal rate of COD presented decreasing tendency, respectively. For example, when the pH was 3, the decolorization rate of C.I. Acid Blue 25 was higher than 95% at 4 min, and the removal rate of COD reached 72.44% at 20 min. Thus, it could be seen that the decolorization rate of C.I. Acid Blue 25 and the removal rate of COD were obvious under the acid condition in O_3/Fenton system.

3.2.2. Effect of mole ratio of $[H_2O_2]/[Fe^{2+}]$

The effects of different mole ratio of $[H_2O_2]/[Fe^{2+}]$ on the O_3/Fenton combination treatment were seen in Fig. 3(b). As the mole ratio of $[H_2O_2]/[Fe^{2+}]$ increased, the decolorization rate of C.I. Acid Blue 25 and the removal rate of COD increased at the beginning and dropped later. Thus, it could be seen that the mole ratio of $[H_2O_2]/[Fe^{2+}]$ affected the decolorization rate of C.I. Acid Blue 25 and the removal rate of COD. When the mole ratio of $[H_2O_2]/[Fe^{2+}]$ was 40:1, the decolorization rate of C.I. Acid Blue 25 and the removal rate of COD were the highest. The decolorization rate of C.I. Acid Blue 25 reached 98.73% at 4 min. In addition, the removal rate of COD reached 89.15% at 20 min. Therefore, the decolorization rate of C.I. Acid Blue 25 and the removal rate of COD were the highest when the mole ratio of $[H_2O_2]/[Fe^{2+}]$ was 40:1.

3.2.3. Effect of initial concentration of AB25

The effects of different initial concentration on the O_3/Fenton combination technology treatment were seen in Fig. 3(c). As the initial concentration of C.I. Acid Blue 25 increased, the decolorization rate of C.I. Acid Blue 25 and the removal rate of COD showed the tendency of decrease. At 4 min, when the initial concentration of C.I. Acid Blue 25 was 20 $mg.L^{-1}$, the decolorization rate of C.I. Acid Blue 25 reached 99.64%, which was higher than the decolorization rate of other initial concentration. However, the differences were not obvious between 20 and 50 $mg.L^{-1}$. The removal rate of COD reached 75.48% when the reaction time was 20 min. Therefore, it could be seen that it was better for the degradation of C.I. Acid Blue 25 and removal rate of COD by O_3/Fenton system under low concentration.

3.2.4. Effect of ozone flux

The effects of different ozone flux on O_3/Fenton combination technology treatment were seen in Fig. 3(d). As the ozone flux increased, the decolorization rate of C.I. Acid Blue 25 and the removal rate of COD both showed the tendency of increase. When the reaction time was 4 min, the decolorization rate of C.I. Acid Blue 25 reached 98.88% at ozone flux of 52 $L.h^{-1}$, and it was a little higher than 98.66% at ozone flux of 36 $L.h^{-1}$. Therefore, continuously increasing the ozone flux was not meaningful for the further promotion of the decolorization rate of C.I. Acid Blue 25. When ozone flux was 60 $L.h^{-1}$, the removal rate of COD reached 86.37% at 20 min. It followed that O_3/Fenton combination technology was more helpful for the decolorization rate of C.I. Acid Blue 25 and the removal rate of COD when the ozone flux was increased.

3.3. Optimization analysis on the degradation of C.I. Acid Blue 25 by RSM

3.3.1. The selections of factors and test plans

O_3/Fenton combination technology was used to deal with the simulated wastewater of C.I. Acid Blue 25. The effects of degradation by initial pH, mole ratio of $[H_2O_2]/[Fe^{2+}]$ and initial concentration ozone flux were studied, and X_1, X_2, X_3 and X_4 were adopted to represent them, respectively. –1, 0, and 1

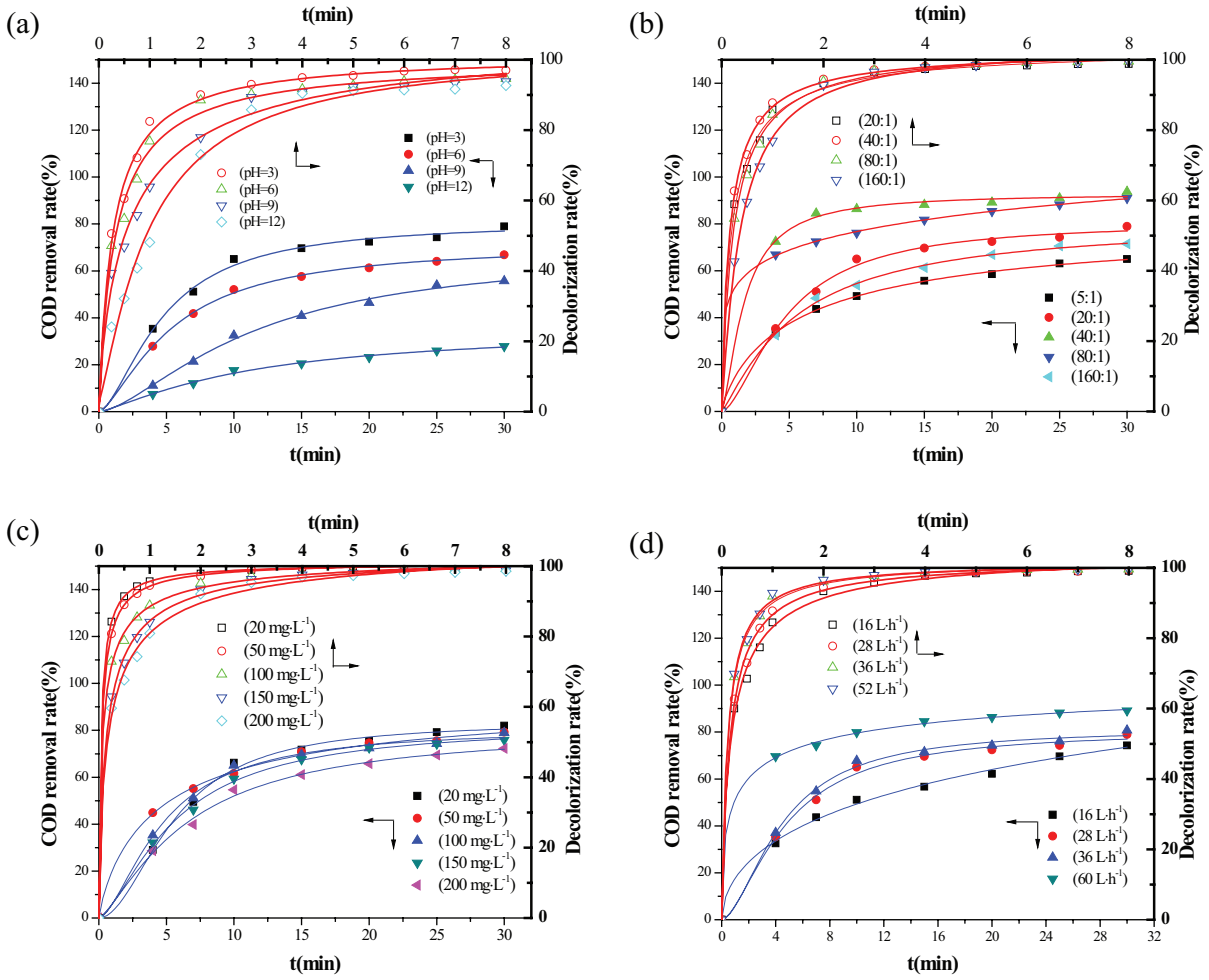

Fig. 3. Effects of factors on the decolorization rate of C.I. Acid Blue 25 and removal rate of COD: (a) initial pH: c_0 = 100 mg.L^{-1}, [H_2O_2]/[Fe^{2+}] = 40:1, $q_{(O3)}$ = 28 L.h^{-1}, T = 298 K; (b) mole rate [H_2O_2]/[Fe^{2+}]: c_0 = 100 mg.L^{-1}, pH = 3, $q_{(O3)}$ = 28 L.h^{-1}, T = 298 K; (c) initial concentration: pH = 3, [H_2O_2]/[Fe^{2+}] = 40:1, $q_{(O3)}$ = 28 L.h^{-1}, T = 298 K; and (d) ozone flux: pH = 3, c_0 = 100 mg.L^{-1}, [H_2O_2]/[Fe^{2+}] = 40:1, T = 298 K.

were chosen as low, medium and high level of the independent variables [35], and the decolorization rate of C.I. Acid Blue 25 was used as response values.

The main effects and interactions of the decolorization rate of C.I. Acid Blue 25 by four factors involving initial concentration, initial pH, mole ratio of [H_2O_2]/[Fe^{2+}] and ozone flux were analyzed. BBD was utilized to design the optimization experiment, and five parallel experiments under the condition of the center value were conducted. Experimental range and levels of independent variables were listed in Table 1. The experiments were operated at room temperature for 4 min, and the decolorization rates of C.I. Acid Blue 25 were measured. By building the model, the optimal conditions of O_3/Fenton combination technology dealing with C.I. Acid Blue 25 in the limited range could be achieved.

3.3.2. The establishment of the model equation and significant analysis

The results of Box-Behnken experiment about degradation of C.I. Acid Blue 25 were listed in Table 2. Design-Expert 8.0 was used to analyze the results of Table 2. The four significantly independent variables (X_1, X_2, X_3 and X_4) and the mathematical relationship describing the response of these variables could be approximated by the following quadratic polynomial equation:

$$\eta = 94.37 - 3.94X_1 - 1.26X_2 - 1.71X_3 + 4.1X_4 - 0.60X_1X_2 + 1.35X_1X_3 + 2.41X_1X_4 + 0.13X_2X_3 - 0.47X_2X_4 + 1.28X_3X_4 + 0.11X_1^2 - 1.62X_2^2 - 0.66X_3^2 - 3.03X_4^2 \quad (2)$$

From Table 3, the effects of the independent variables X_1, X_3, X_4, X_1X_4 and X_4^2 were obvious (p values < 0.05). That was to say, the square effect of ozone flux was obvious while the effects of other factors were not obvious. The p value was 0.0001 via variance analysis, and it showed that the effects were very obvious. The results of variance analysis showed that the order of the four influence factors was ozone flux > initial pH > initial concentration > mole ratio of [H_2O_2]/[Fe^{2+}]. The measured values were close to the

Table 2
Box-Behnken design experiments and experimental results

Run	Coded levels				Decolorization rate (η)	
	X_1	X_2	X_3	X_4	Actual, %	Predicted, %
1	–1	0	1	0	96.44	94.69
2	1	0	1	0	91.07	89.51
3	0	0	–1	–1	90.25	89.57
4	0	0	0	0	94.27	94.37
5	0	–1	0	1	93.93	95.55
6	0	0	0	0	94.48	94.37
7	0	–1	1	0	89.14	91.50
8	0	–1	0	–1	87.12	86.41
9	0	1	0	–1	86.84	84.83
10	0	0	1	1	95.35	94.34
11	1	1	0	0	88.77	87.05
12	0	1	1	0	87.10	89.24
13	0	1	–1	0	92.70	92.41
14	1	0	0	1	92.18	94.01
15	0	1	0	1	91.77	92.09
16	0	–1	–1	0	95.27	95.19
17	0	0	–1	1	96.70	95.22
18	–1	–1	0	0	97.41	97.45
19	0	0	0	0	93.93	94.37
20	–1	1	0	0	94.57	96.14
21	0	0	0	0	94.55	94.37
22	–1	0	0	–1	93.46	93.70
23	0	0	1	–1	83.79	83.59
24	–1	0	0	1	98.36	97.08
25	1	–1	0	0	94.02	90.78
26	1	0	–1	0	88.89	90.24
27	1	0	0	–1	77.64	81.00
28	–1	0	–1	0	99.64	100.81
29	0	0	0	0	94.61	94.37

predicted values. Therefore, the model could be used to optimize the degradation. The coefficient of variation was 2.39%. It indicated that the credibility and precision of the experiment were high.

3.3.3. The response surface analysis of interaction factors of degradation

3.3.3.1. The interactions between initial pH and mole ratio of $[H_2O_2]/[Fe^{2+}]$ The response surface and contour plots of the effects between initial pH and mole ratio of $[H_2O_2]/[Fe^{2+}]$ on the decolorization rate of the C.I. Acid Blue 25 were seen in Fig. 4. The interactions between initial pH and mole ratio of $[H_2O_2]/[Fe^{2+}]$ were not obvious. However, because the slope of the curved surface of initial pH was greater than that of mole ratio of $[H_2O_2]/[Fe^{2+}]$, the effect of initial pH on the decolorization rate of C.I. Acid Blue 25 was greater than that of mole ratio of $[H_2O_2]/[Fe^{2+}]$. As it was seen in Fig. 4(b), the mole ratio of $[H_2O_2]/[Fe^{2+}]$ kept invariable; the decolorization rate of C.I. Acid Blue 25 increased with the decreasing of the pH value. The degradation effects in acid condition were significantly higher than those in alkaline condition.

Table 3
ANOVA results of removal rate for C.I. Acid Blue 25 using O_3/Fenton process

Source	Sum of squares	Degrees of freedom	Mean square	*F* value	*p* value	
Model	553.61	14	39.5	8.86	0.0001	Significant
X_1	186.38	1	186.38	41.74	<0.0001	
X_2	19.1	1	19.1	4.28	0.0577	
X_3	35.2	1	35.2	7.89	0.0139	
X_4	201.76	1	201.76	45.18	<0.0001	
X_1X_2	1.45	1	1.45	0.32	0.5778	
X_1X_3	7.25	1	7.25	1.62	0.2232	
X_1X_4	23.2	1	23.2	5.19	0.0389	
X_2X_3	0.068	1	0.068	0.015	0.9036	
X_2X_4	0.89	1	0.89	0.2	0.6623	
X_3X_4	6.52	1	6.52	1.46	0.2470	
X_1^2	0.072	1	0.072	0.016	0.9009	
X_2^2	17	1	17	3.82	0.0710	
X_3^2	2.84	1	2.84	0.64	0.4386	
X_4^2	59.5	1	59.5	13.31	0.0026	

Note: $R^2 = 0.8985$.

3.3.3.2. The interactions between initial concentration and ozone flux The interactions between initial concentration and ozone flux were obvious in Fig. 5. Because the slope of curved surface of ozone flux was greater than that of the initial concentration, the effect of initial concentration on the decolorization rate of C.I. Acid Blue 25 was greater than that of ozone flux. From Fig. 4, it meant that when the initial pH and mole ratio of $[H_2O_2]/[Fe^{2+}]$ were at the center value, and initial concentration kept in a certain degree; the decolorization rate of C.I. Acid Blue 25 increased as the ozone flux increased. When ozone flux reached 38 $L.h^{-1}$, the increasing rate slowed down. As a result, ozone would give priority to reacting with the pollutant that reacted fast. Therefore, it demonstrated that ozone oxidation had certain selectivity. The pollutants that reacted slowly were hard to be treated [22].

3.3.3.3. The interactions between initial pH and initial concentration Fig. 6 showed that the interactions between initial pH and concentration were obvious. Because the slope of curved surface of initial pH was obviously greater than that of initial concentration, the effects of initial pH on the decolorization rate of C.I. Acid Blue 25 were greater than that of initial concentration. When the initial concentration kept invariable, the decolorization rate of C.I. Acid Blue 25 increased with the decrease of pH. Zhu et al. [27] put forward that the efficiency was affected because of high pH. H_2O_2 in

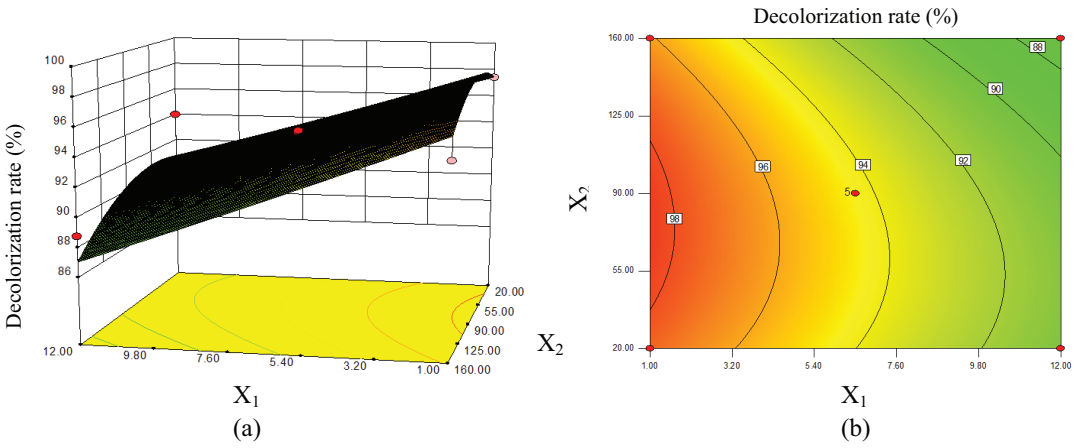

Fig. 4. Response surface (a) and contour plots (b) for the degradation effect of C.I. Acid Blue 25 vs. experimental initial pH (X_1) and mole ratio of $[H_2O_2]/[Fe^{2+}]$ (X_2). Actual factor: c_0 = 110 mg.L^{-1} and $q_{(O3)}$ = 38 L.h^{-1}, 4 min treatment.

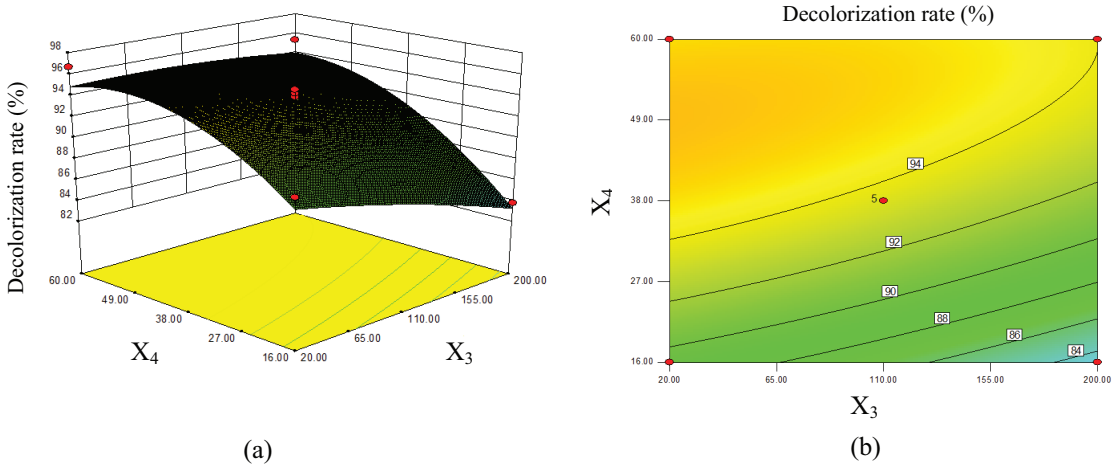

Fig. 5. Response surface (a) and contour plots (b) for the degradation effect of C.I. Acid Blue 25 vs. experimental initial dye concentration (X_3) and ozone flux (X_4). Actual factor: pH = 6.50 and $[H_2O_2]/[Fe^{2+}]$ = 90:1, 4 min treatment.

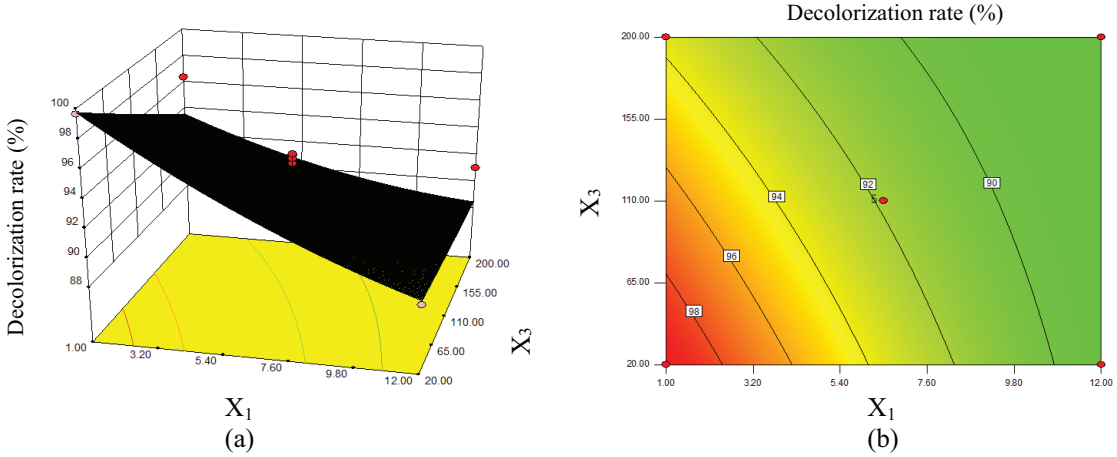

Fig. 6. Response surface (a) and contour plots (b) for the degradation effect of C.I. Acid Blue 25 vs. experimental initial pH (X_1) and dye concentration (X_3). Actual factor: $[H_2O_2]/[Fe^{2+}]$ = 90:1 and $q_{(O3)}$ = 38 L.h^{-1}, 4 min treatment.

Fenton was decomposed too fast at high pH, which caused that organic matter could not be oxidized effectively.

3.3.3.4. The interactions between mole ratio of $[H_2O_2]/[Fe^{2+}]$ and ozone flux As could be seen in Fig. 7, when initial pH and initial concentration were at center value, and the mole ratio of $[H_2O_2]/[Fe^{2+}]$ increased, the decolorization rate of C.I. Acid Blue 25 increased at the beginning and dropped later. The optimal value of the mole ratio of $[H_2O_2]/[Fe^{2+}]$ was about 50:1. The existence of Fe^{2+} could accelerate the generation of ·OH. However, hydroxyl radicals would be captured by the reaction with the surplus Fe^{2+}. In addition, the formed Fe^{3+} could react with H_2O_2 to generate Fe^{2+} and hydroperoxyl radicals (HO_2·) in solution [36–38]. Because the H_2O_2 was consumed, it made the oxidization inefficient. Therefore, there must be an optimal value of mole ratio of $[H_2O_2]/[Fe^{2+}]$ in the Fenton oxidizing technology.

3.3.3.5. The interactions between initial pH and ozone flux Fig. 8 illustrated that the effects of initial pH on the decolorization rate of C.I. Acid Blue 25 were smaller than that of ozone flux. The decolorization rate of C.I. Acid Blue 25 decreased with the increase of the initial pH. The pH was a significant factor affecting the Fenton reaction. Klamerth et al. [39] reported that high degradation efficiency could be obtained when pH was 3 in photo-Fenton. The results above corresponded with the optimized result in this paper. Similarly, high degradation efficiency was also obtained at pH 3 in O_3/Fenton. At the mole ratio of $[H_2O_2]/[Fe^{2+}]$ of 90:1 and ozone flux of 38 $L.h^{-1}$, the decolorization rate of C.I. Acid Blue 25 increased as pH decreased when the initial concentration kept invariable. As could be seen from Fig. 8, when the pH was low (2–4), the decomposition rate of H_2O_2 increased slowly. The Fenton reaction also played an important role in oxidizing pollutants. Thus, higher treatment efficiency could be obtained at relatively low pH.

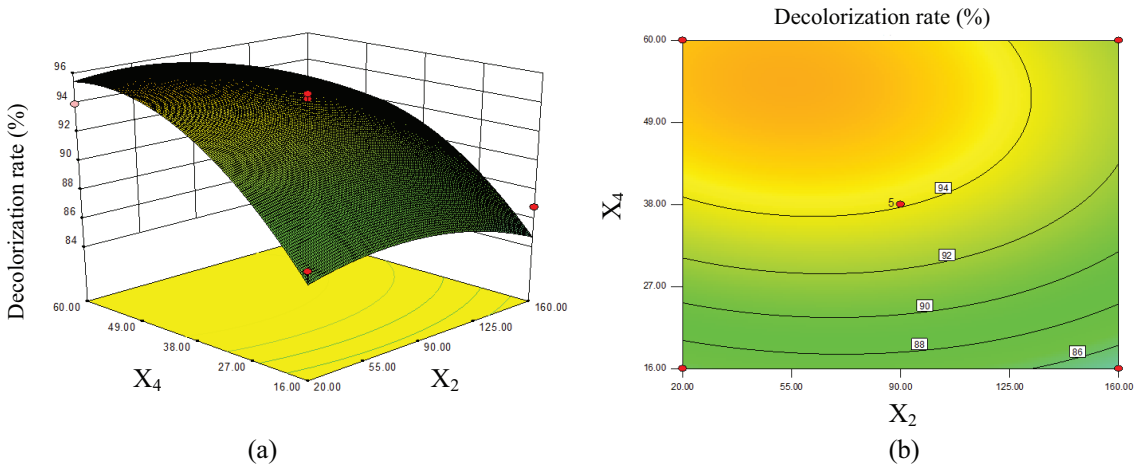

Fig. 7. Response surface (a) and contour plots (b) for the degradation effect of C.I. Acid Blue 25 vs. experimental mole ratio of $[H_2O_2]/[Fe^{2+}]$ (X_2) and ozone flux (X_4). Actual factor: pH = 6.50 and c_0 = 110 mg.L^{-1}, 4 min treatment.

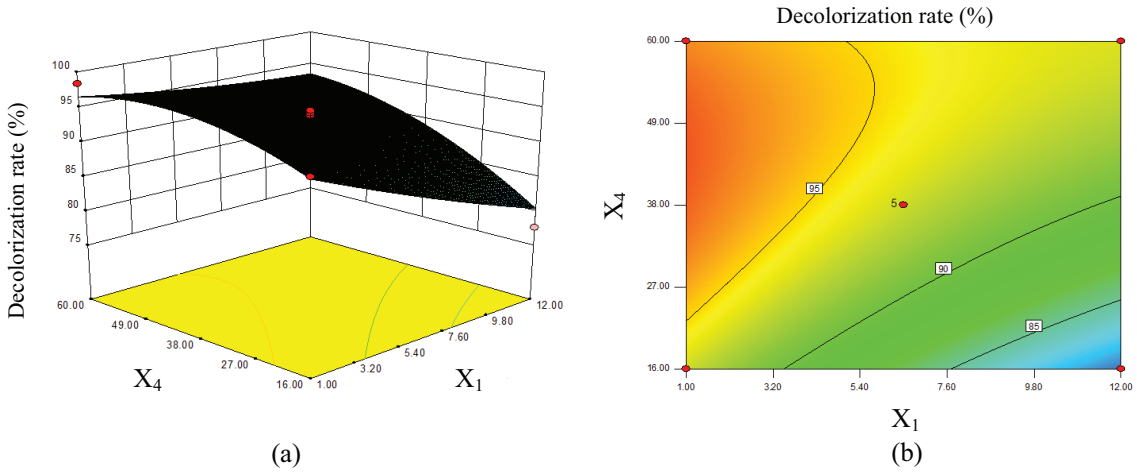

Fig. 8. Response surface (a) and contour plots (b) for the degradation effect of C.I. Acid Blue 25 vs. experimental initial pH (X_1) and ozone flux (X_4). Actual factor: $[H_2O_2]/[Fe^{2+}]$ = 90:1 and c_0 = 110 mg.L^{-1}, 4 min treatment.

3.3.3.6. The interactions between mole ratio of $[H_2O_2]/[Fe^{2+}]$ and initial concentration Fig. 9 showed that the slope of response surface of initial concentration was greater than that of mole ratio of $[H_2O_2]/[Fe^{2+}]$. Thus, the effect of initial concentration on the decolorization rate of C.I. Acid Blue 25 was more obvious than that of mole ratio of $[H_2O_2]/[Fe^{2+}]$ during degradation process. When initial pH and ozone flux were at the center value, as the mole ratio of H_2O_2 increased, the decolorization rate of C.I. Acid Blue 25 showed a tendency of increase at the beginning and decrease later. Little amount of $FeSO_4.7H_2O$ was not beneficial to generate ·OH during the degradation process. Thus, the catalytic activity was restricted. In contrast, if the additive amount of $FeSO_4.7H_2O$ was too much, Fe^{2+} would be oxidized to generate Fe^{3+}, which led to form precipitation. And the catalytic effect was also reduced. Therefore, when the mole ratio of $[H_2O_2]/[Fe^{2+}]$ was 40:1, it could be helpful for the catalysis.

3.3.4. Verification experiment

Considering the degradation efficiency and processing cost comprehensively, the Design Expert software was used to study optimal research. As could be seen in Table 4, the decolorization rate of C.I. Acid Blue 25 was 96.67% at 4 min in O_3/Fenton system under the optimal conditions that pH of 5.48, $[H_2O_2]/[Fe^{2+}]$ of 45.47, c_0 of 55.08 mg.L^{-1} and q of 42.06 L.h^{-1}. By validating the results by parallel experiment, the decolorization rate was 96.39%, and the deviation with the model prediction was only 2.90%.

3.4. Mechanism analysis of C.I. Acid Blue 25

3.4.1. Possible degradation pathway

Intermediate products were detected by GC/MS during the degradation process. UV-Vis and FT-IR analyses as assisted technique were used to study degradation mechanism during the oxidation process. The GC/MS chromatogram of intermediates of C.I. Acid Blue 25 in O_3/Fenton degradation system could be seen in Supplementary material. Based on the study above, a plausible mineralization pathway and main intermediate products for degradation of C.I. Acid Blue 25 by O_3/Fenton system were illustrated in Fig. 10. Decomposition of C.I. Acid Blue 25 was firstly initiated by the cleavage of –C–N– and was cleavaged into 1-amino anthraquinone (A_1), aniline (B_1) and Na_2SO_4 as possible intermediates. Owing to the attacks of hydrogen radical and the oxidization, A_1 was turned into 1-hydroxy anthraquinone (A_2). Under the influence of the ·OH and aqueous solution, A_2 was then transformed into compound 1,3-indanedione (A_3). Then A_3 was oxidized into phthalic acid (A_4); finally, A_4 was degraded into CO_2 and H_2O. B_1 was transformed into phenol (B_2). B_2 was turned into the compound hydroquinone (B_3) or catechol (B_4). B_3 or B_4 could be converted into *p*-benzoquinone (B_5). The ring C=C of B_5 was broken down into the compound maleic acid (B_6). B_6 was turned into oxalic acid (B_7), and B_7 was oxidized into formic acid (B_8). Finally, B_8 was degraded into CO_2 and H_2O [40].

3.4.2. Mechanism analysis of main intermediates

Degradation of C.I. Acid Blue 25 was considered to proceed according to ionic/radical mechanism of O_3/Fenton. Alternative pathways may be tried to explain the formation of some species [40]. The first process was showed in Fig. 11(a) that the C.I. Acid Blue 25 underwent the "Bucherer reaction" and was degraded into some species that included A_1 and B_1. From Fig. 11(b), the second process illustrated that A_2 could be generated as result of a direct ozone attack or due to a hydroxyl radical attack on A_1. It could be seen from Fig. 11(c) that A_3 could be formed through an attack of the hydroxyl radical on supposed ring cleavage of A_2 in third process. The fourth process in Fig. 11(d) showed that A_4 could be formed through an attack of the hydroxyl radical on supposed ring cleavage of A_3 followed by a decarboxylation reaction. The successive oxidation of A_4 produced carbon dioxide and water [41]. As could be seen from Fig. 11(e), in the fifth process, B_2 could be formed through an attack of the hydroxyl radical on B_1. Similarly,

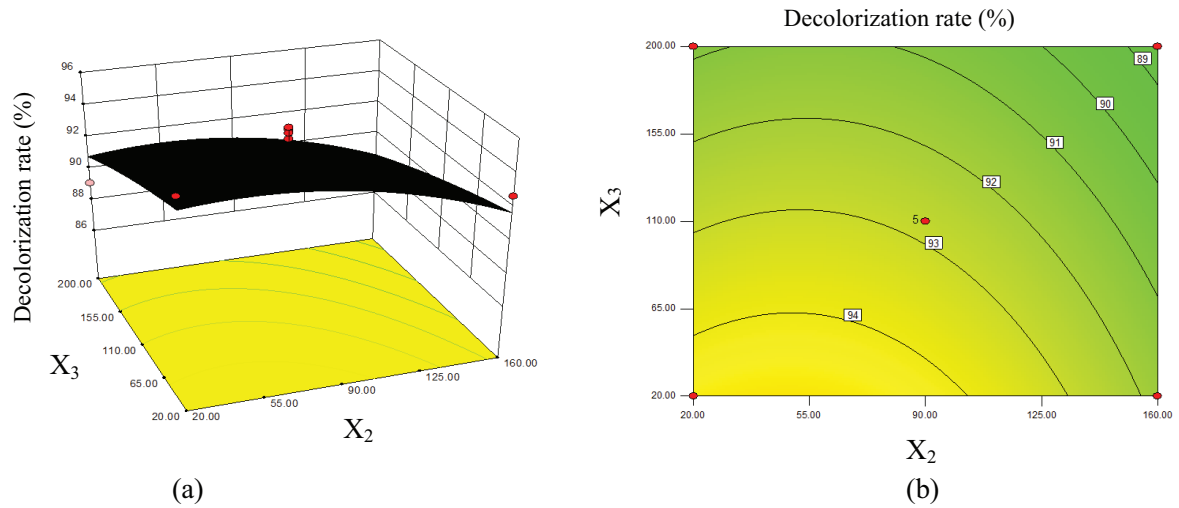

Fig. 9. Response surface (a) and contour plots (b) for the degradation effect of C.I. Acid Blue 25 vs. experimental mole ratio of $[H_2O_2]/[Fe^{2+}]$ (X_2) and initial dye concentration (X_3). Actual factor: pH = 6.50 and $q_{(O3)}$ = 38 L.h^{-1}, 4 min treatment.

Table 4
The optimum condition for degradation on C.I. Acid Blue 25

Number	pH	Mole ratio	Initial concentration ($mg.L^{-1}$)	Ozone flux ($L.h^{-1}$)	Decolorization rate, %	
1	6.5	90	110	38	94.3695	
2	6.5	90	200	16	83.5904	
3	6.5	20	20	38	95.1919	
4	6.5	90	20	16	89.5696	
5	6.5	20	110	16	86.4105	
6	6.5	20	200	38	91.5047	
7	5.06	78.78	24.4	16.42	91.733	
8	6.41	68.95	118.51	24.39	90.6606	
9	5.16	49.48	129.49	40.33	95.3467	
10	6.59	56.51	31.54	41.22	95.9763	
11	5.48	45.47	55.08	42.06	96.6664	Selected
12	6.33	76.28	137.13	23.72	89.8803	
13	8.95	27.07	36.27	35.51	92.7134	
14	7.89	51.89	181.82	28.72	89.0315	
15	5.56	95.01	113.77	29.46	92.9726	
16	5.19	56.89	121.76	38.58	95.2943	
17	6.25	76.35	118.68	17.24	87.8865	
18	9.75	28.56	196.05	24.94	85.3432	
19	9.26	51.76	193.03	29.81	88.2695	
20	4.21	34.89	113.73	41.66	96.2251	
21	8.47	66.31	155.81	47.01	94.321	
22	8.42	58.32	129.53	44.06	94.2916	
23	9.99	96.72	134.43	32.78	89.8814	
24	9.08	65.4	82.19	33.73	92.0885	
25	6.51	47.88	148.57	27.16	90.4792	
26	5.22	86.78	145.02	37.26	94.3076	
27	8.56	41.99	38.32	45	94.8436	
28	4.66	57.25	111.98	48.7	96.8010	
29	9.04	24	130.63	39.58	92.6810	
30	5.8	20.83	53.62	20.2	90.6839	
31	7.9	97.24	37.87	31.72	92.5861	
32	6.86	31.26	185.58	20.39	85.6154	
33	5.45	63.48	39.8	19.31	91.9215	
34	6.36	73.57	158.46	48.01	95.0975	
35	7.72	52.02	154.52	33.49	91.6243	
36	6.56	77.66	141.5	35	93.1249	

the formed B_3 and B_4 could be regarded as result of a direct ozone attack or as due to hydroxyl radical attacking on B_2. The sixth process was showed in Fig. 11(f). The intermediate products M_1 could be formed through an "anomalous ozonation" of B_5, the decarboxylation of supposed α-keto acid intermediate products M_1 could be used to explain the formation of B_6. B_7 was generated after B_6 underwent the successive repetition reaction (1) and (2). Then B_7 was degraded into carbon dioxide and water [42]. From Fig. 11(g), the seventh process suggested that the formed B_7 could be reported as result of a direct ozone attack or as due to hydroxyl radical attacking on B_4 followed by oxidization.

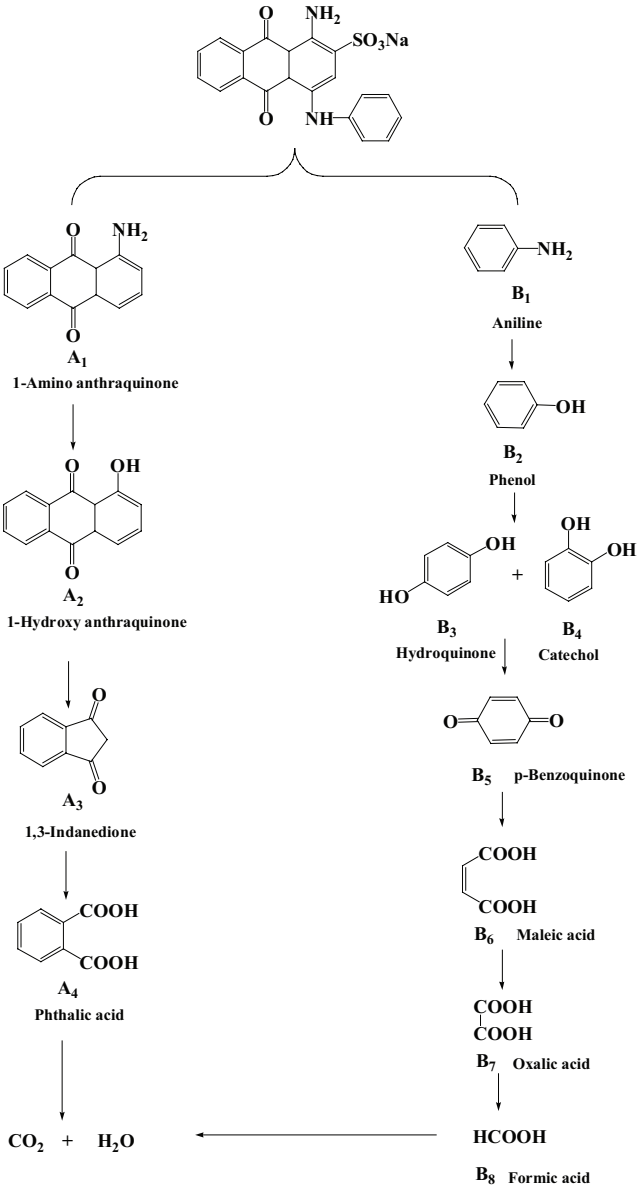

Fig. 10. The possible degradation pathway of C.I. Acid Blue 25 by O_3/Fenton.

3.5. Comparison of works by different AOPs

The comparative table, where the trend of studies done by different AOPs was displayed, has been presented. The comparisons of degradation for C.I. Acid Blue 25 on different AOPs were showed in Table 5. Ghodbane and Hamdaoui [43] reported that the decolorization rates of C.I. Acid Blue 25 reached 84% and 70% under UV/H_2O_2 and UV/Fe^{2+} after 8 min. In the study of Grcic et al. [44], when UV/Fenton system was applied to treat C.I. Acid Blue 25, more than 90% of total organic carbon (TOC) and 100% of decolorization rate were obtained after 60 min. However, in our paper, the complete decolorization could be received after 5 min, and 79 % of COD removal rate was obtained after 20 min in by O_3/Fenton system. By comparison, the O_3/Fenton system has higher treating efficiency to degradation of C.I. Acid Blue 25

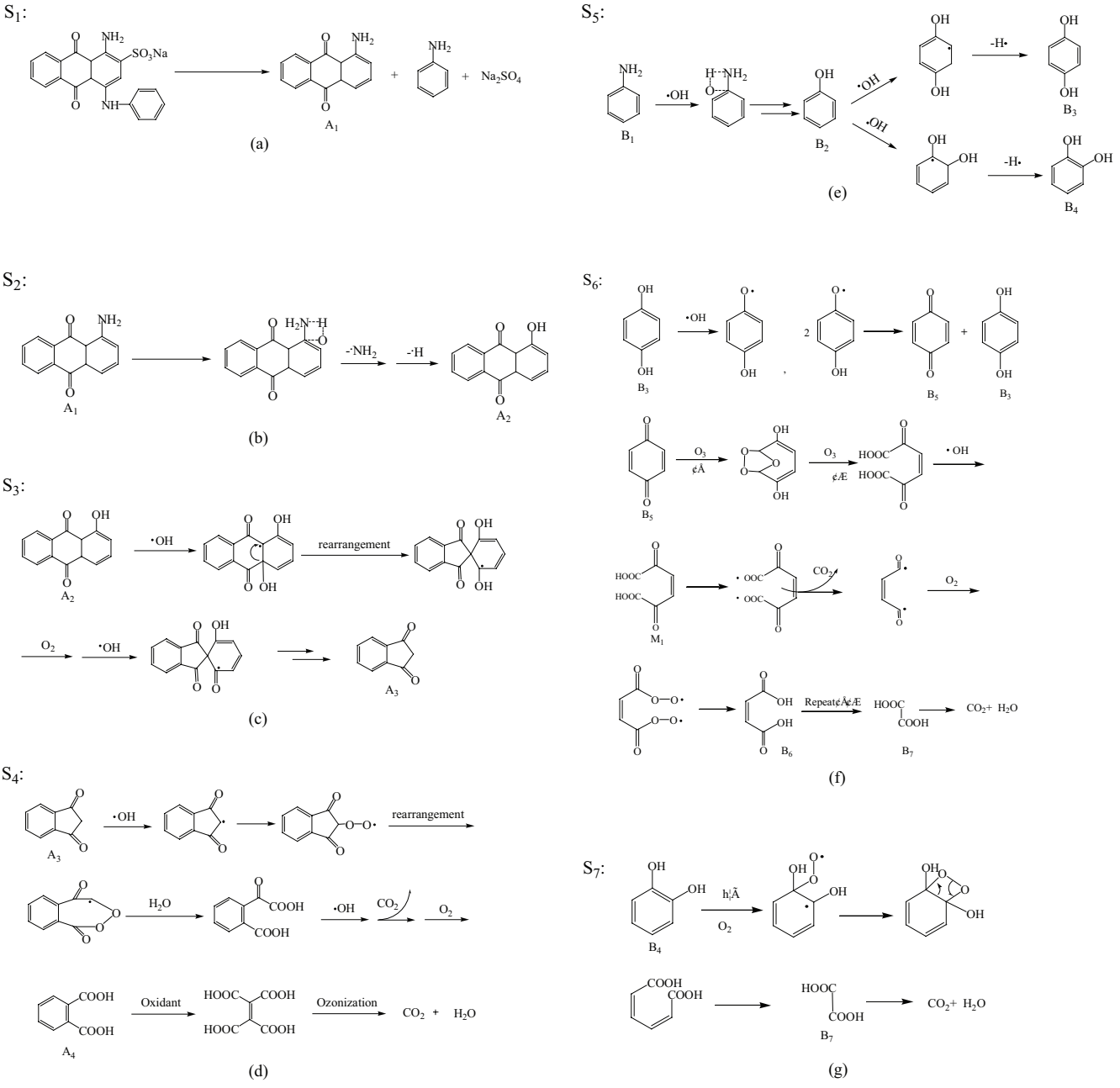

Fig. 11. Mechanism analysis of main intermediates.

in shorter time. The paper also indicated that O_3/Fenton system, which was a developing technology, deserved further study.

4. Conclusions

In this paper, the complete decolorization for C.I. Acid Blue 25 in O_3/Fenton system could be obtained, and the highest removal rate of COD reached 89.15% at 20 min. Then BBD experiment and response surface analysis were used to study each influence factor. The order of interaction factors of degradation was ozone flux > pH > mole ratio of $[H_2O_2]/[Fe^{2+}]$. Under the optimum conditions that pH of 5.48, $[H_2O_2]/[Fe^{2+}]$ of 45.47, c_0 of 55.08 mg.L^{-1} and $q_{(O3)}$ of 42.06 L.h^{-1}, the decolorization rate reached 6.67%, and the deviation with the model prediction was 2.90%.

By UV-Vis, FT-IR and GC/MS analyses, important intermediates such as *p*-benzoquinone, aniline, catechol, hydroquinone, 1-amino anthraquinone and 1-hydroxy anthraquinone could be obtained. The alternative pathways of intermediates were proposed first and explained the degradation process in detail. Degradation process of C.I. Acid Blue 25 indicated that both direct molecular ozone reaction and indirect radical reaction were involved in the O_3/Fenton

Table 5
The comparisons of degradation for C.I. Acid Blue 25 by different AOPs

Technological methods	Conditions	Decolorization rate	Removal rate of COD	Removal rate of TOC	Refs.
O_3/Fenton	pH 3, $[H_2O_2]/[Fe^{2+}]$ 40:1, $q_{(O3)}$ 28 L.h^{-1}, c_0 50 mg.L^{-1}, 298 K and 20 min	100% (5 min)	79%	–	This paper
UV	pH 5.7, c_0 50 mg.L^{-1}, UV irradiation 15 mW.cm^{-2}, 293 K and 20 min	26%	–	–	Ghodbane and Hamdaoui [43]
UV/H_2O_2	pH 5.7, c_0 50 mg.L^{-1}, UV irradiation 15 mW.cm^{-2}, $[H_2O_2]$ 1,543 mg.L^{-1}, 293 K and 8 min	84%	–	–	
UV/Fe^{2+}	pH 3, c_0 50 mg.L^{-1}, UV irradiation 15 mW.cm^{-2}, $[Fe^{2+}]$ 30 mg.L^{-1}, 293 K and 8 min	70%	–	–	
UV/Fenton	pH 3.0, UV I_0 3.42 × 10^{-6} Einstein dm^{-3}s^{-1}, $[Fe^{2+}]$ 0.5 mmol dm^{-3}, $[H_2O_2]$ 2.5 mmol dm^{-3}, c_0 100 mg.L^{-1}, 296 K and 60 min	100%	–	90%	Grcic et al. [44]

–: no data was found.

system. During the tentative degradation, the main intermediates derived from the experiments could be decomposed and oxidized into small molecule acids like oxalic acids, and finally turned into CO_2 and H_2O.

Acknowledgments

The authors gratefully acknowledge the financial support from National Natural Science Foundation of China (No. 21246010) and Jiangsu Eastern Coast and Yangtse River Area Development Institute (Z201402).

References

[1] P. Colindres, H. Yee-Madeira, E. Reguera, Removal of Reactive Black 5 from aqueous solution by ozone for water reuse in textile dyeing processes, Desalination, 258 (2010) 154–158.
[2] B. Kayan, B. Gozmen, Degradation of Acid Red 274 using H_2O_2 in subcritical water: application of response surface methodology, J. Hazard. Mater., 201 (2012) 100–106.
[3] C. Tizaoui, N. Grima, Kinetics of the ozone oxidation of Reactive Orange 16 azo-dye in aqueous solution, Chem. Eng. J., 173 (2011) 463–473.
[4] X.B. Zhang, W.Y. Dong, W. Yang, Decolorization efficiency and kinetics of typical reactive azo dye RR2 in the homogeneous Fe(II) catalyzed ozonation process, Chem. Eng. J., 233 (2013) 14–23.
[5] C.L. Yang, J. McGarrahan, Electrochemical coagulation for textile effluent decolorization, J. Hazard. Mater., 127 (2005) 40–47.
[6] P.C.C. Faria, J.J.M. Orfao, M.F.R. Pereira, Adsorption of anionic and cationic dyes on activated carbons with different surface chemistries, Water Res., 38 (2004) 2043–2052.
[7] E.N. El Qada, S.J. Allen, G.M. Walker, Adsorption of methylene Blue onto activated carbon produced from steam activated bituminous coal: a study of equilibrium adsorption isotherm, Chem. Eng. J., 124 (2006) 103–110.
[8] K. Sarayu, S. Sandhya, Current technologies for biological treatment of textile wastewater—a review, Appl. Biochem. Biotech., 167 (2012) 645–661.
[9] Y.Y. Li, T. Noike, Upgrading of anaerobic digestion of waste activated sludge by thermal pretreatment, Water Sci. Technol., 26 (1992) 857–866.
[10] E. Chatzisymeon, N.P. Xekoukoulotakis, A. Coz, N. Kalogerakis, D. Mantzavinos, Electrochemical treatment of textile dyes and dyehouse effluents, J. Hazard. Mater., 137 (2006) 998–1007.
[11] M. Panizza, G. Cerisola, Removal of colour and COD from wastewater containing Acid Blue 22 by electrochemical oxidation, J. Hazard. Mater., 153 (2008) 83–88.
[12] K. Singh, S. Arora, Removal of synthetic textile dyes from wastewaters: a critical review on present treatment technologies, Crit. Rev. Env. Sci. Tec., 41 (2011) 807–878.
[13] M. Jonstrup, M. Punzi, B. Mattiasson, Comparison of anaerobic pre-treatment and aerobic post-treatment coupled to photo-Fenton oxidation for degradation of azo dyes, J. Photochem. Photobiol., A, 224 (2011) 55–61.
[14] M. Mehrjouei, S. Muller, D. Moller, Energy consumption of three different advanced oxidation methods for water treatment: a cost-effectiveness study, J. Clean. Prod., 65 (2014) 178–183.
[15] N.N. Mahamuni, Y.G. Adewuyi, Advanced oxidation processes (AOPs) involving ultrasound for waste water treatment: a review with emphasis on cost estimation, Ultrason. Sonochem., 17 (2010) 990–1003.
[16] Y.J. Shen, L.C. Lei, X.W. Zhang, M.H. Zhou, Y. Zhang, Effect of various gases and chemical catalysts on phenol degradation pathways by pulsed electrical discharges, J. Hazard. Mater., 150 (2008) 713–722.
[17] H. Yu, E. Nie, J. Xu, S.W. Yan, W.J. Cooper, W.H. Song, Degradation of diclofenac by advanced oxidation and reduction processes: kinetic studies, degradation pathways and toxicity assessments, Water Res., 47 (2013) 1909–1918.
[18] C. Comninellis, A. Kapalka, S. Malato, S.A. Parsons, I. Poulios, D. Mantzavinos, Advanced oxidation processes for water treatment: advances and trends for R&D, J. Chem. Technol. Biotechnol., 83 (2008) 769–776.
[19] L. Sun, S.G. Wan, Z.B. Yu, L.J. Wang, Optimization and modeling of preparation conditions of TiO_2 nanoparticles coated on hollow glass microspheres using response surface methodology, Sep. Purif. Technol., 125 (2014) 156–162.
[20] J.J. Wu, J.S. Yang, M. Muruganandham, C.C. Wu, The oxidation study of 2-propanol using ozone-based advanced oxidation processes, Sep. Purif. Technol., 62 (2008) 39–46.
[21] H.W. Chen, Y.L. Kuo, C.S. Chiou, S.W. You, C.M. Ma, C.T. Chang, Mineralization of reactive black 5 in aqueous solution by ozone/H_2O_2 in the presence of a magnetic catalyst, J. Hazard. Mater., 174 (2010) 795–800.

[22] D.H. Bremner, S. Di Carlo, A.G. Chakinala, G. Cravotto, Mineralisation of 2,4-dichlorophenoxyacetic acid by acoustic or hydrodynamic cavitation in conjunction with the advanced Fenton process, Ultrason. Sonochem., 15 (2008) 416–419.
[23] V.J. Pereira, K.G. Linden, H.S. Weinberg, Evaluation of UV irradiation for photolytic and oxidative degradation of pharmaceutical compounds in water, Water Res., 41 (2007) 4413–4423.
[24] Y.J. Shen, Q.H. Xu, R.R. Wei, J.L. Ma, Y. Wang, Mechanism and dynamic study of reactive red X-3B dye degradation by ultrasonic-assisted ozone oxidation process, Ultrason. Sonochem. (2016). doi: 10.1016/j.ultsonch.2016.08.006
[25] Y.J. Shen, S. Han, Q.H. Xu, Y. Wang, Z.Y. Xu, B. Zhao, R.P. Zhang, Optimizing degradation of Reactive Yellow 176 by dielectric barrier discharge plasma combined with TiO_2 nano-particles prepared using response surface methodology, J. Taiwan Inst. Chem. Eng., 60 (2016) 302–312.
[26] Y.J. Shen, L.C. Lei, X.W. Zhang, J.D. Ding, Degradation of acid orange 7 dye in two hybrid plasma discharge reactors, Plasma Sci. Technol., 16 (2014) 1020–1031.
[27] X.B. Zhu, J.P. Tian, R. Liu, L.J. Chen, Optimization of Fenton and electro-Fenton oxidation of biologically treated coking wastewater using response surface methodology, Sep. Purif. Technol., 81 (2011) 444–450.
[28] H.Y. Li, Y.L. Li, L.J. Xiang, Q.Q. Huang, J.J. Qiu, H. Zhang, M.V. Sivaiah, F. Baron, J. Barrault, S. Petit, S. Valange, Heterogeneous photo-Fenton decolorization of Orange II over Al-pillared Fe-smectite: response surface approach, degradation pathway, and toxicity evaluation, J. Hazard. Mater., 287 (2015) 32–41.
[29] A. López-López, J.S. Pic, H. Debellefontaine, Ozonation of azo dye in a semi-batch reactor: a determination of the molecular and radical contributions, Chemosphere, 66 (2007) 2120–2126.
[30] S.S. Moghaddam, M.R. Alavi Moghaddam, M. Arami, Response surface optimization of acid red 119 dye from simulated wastewater using Al based waterworks sludge and polyaluminium chloride as coagulant, J. Environ. Manage., 92 (2011) 1284–1291.
[31] M.C. Martí-Calatayud, M.C. Vincent-Vela, S. Álvarez-Blanco, J. Lora-García, E. Bergantiños-Rodríguez, Analysis and optimization of the influence of operating conditions in the ultrafiltration of macromolecules using a response surface methodological approach, Chem. Eng. J., 156 (2010) 337–346.
[32] Y. Yang, Y. Li, Y.M. Zhang, D.W. Liang, Applying hybrid coagulants and polyacrylamide flocculants in the treatment of high-phosphorus hematite flotation wastewater (HHFW): optimization through response surface methodology, Sep. Purif. Technol., 76 (2010) 72–78.
[33] J.M. Fanchiang, D.H. Tseng, Degradation of anthraquinone dye C.I. Reactive Blue 19 in aqueous solution by ozonation, Chemosphere, 77 (2009) 214–221.
[34] D.Z. Dan, R.C. Sandford, P.J. Worsfold, Determination of chemical oxygen demand in fresh waters using flow injection with on-line UV-photocatalytic oxidation and spectrophotometric detection, Analyst, 130 (2005) 227–232.
[35] P. Tripathi, V.C. Srivastava, A. Kumar, Optimization of an azo dye batch adsorption parameters using Box-Behnken design, Desalination, 249 (2009) 1273–1279.
[36] F.J. Benitez, J.L. Acero, F.J. Real, F.J. Rubio, A.I. Leal, The role of hydroxyl radicals for the decomposition of p-hydroxy phenylacetic acid in aqueous solutions, Water Res., 35 (2001) 1338–1343.
[37] H. Lee, M. Shoda, Removal of COD and color from livestock wastewater by the Fenton method, J. Hazard. Mater., 153 (2008) 1314–1319.
[38] S. Meric, D. Kaptan, T. Ölmez, Color and COD removal from wastewater containing Reactive Black 5 using Fenton's oxidation process, Chemosphere, 53 (2004) 435–441.
[39] N. Klamerth, S. Malato, A. Aguera, A. Fernandez-Alba, Photo-Fenton and modified photo-Fenton at neutral pH for the treatment of emerging contaminants in wastewater treatment plant effluents: a comparison, Water Res., 47 (2013) 833–840.
[40] Z.Q. He, L.L. Lin, S. Song, M. Xia, L.J. Xu, H.P. Ying, J.M. Chen, Mineralization of C.I. Reactive Blue 19 by ozonation combined with sonolysis: performance optimization and degradation mechanism, Sep. Purif. Technol., 62 (2008) 376–381.
[41] M.P. Gao, Z.Q. Zeng, B.C. Sun, H.K. Zou, J.F. Chen, L. Shao, Ozonation of azo dye Acid Red 14 in a microporous tube-in-tube microchannel reactor: decolorization and mechanism, Chemosphere, 89 (2012) 190–197.
[42] C.Y. Zhang, L.J. Yang, F. Rong, D.G. Fu, Z.Z. Gu, Boron-doped diamond anodic oxidation of ethidium bromide: Process optimization by response surface methodology, Electrochim. Acta, 64 (2012) 100–109.
[43] H. Ghodbane, O. Hamdaoui, Decolorization of antraquinonic dye, C.I. Acid Blue 25, in aqueous solution by direct UV irradiation, UV/H_2O_2 and UV/Fe(II) processes, Chem. Eng. J., 160 (2010) 226–231.
[44] I. Grcic, S. Papic, D. Mesec, N. Koprivanac, D. Vujevic, The kinetics and efficiency of UV assisted advanced oxidation of various types of commercial organic dyes in water, J. Photochem. Photobiol. A, 273 (2014) 49–58.

Supplementary material

The GC/MS chromatogram of intermediates of C.I. Acid Blue 25 in O_3/Fenton system.